ASTRONOMY & ASTROPHYSICS
SUPPLEMENT SERIES

JANUARY **1997**, PAGE 45

Astron. Astrophys. Suppl. Ser. **121,** 45-55 (1997)

BVRI photometry of a few 'unidentified' IRAS sources

K.V.K. Iyengar and M. Parthasarathy

Indian Institute of Astrophysics, Bangalore 560 034, India

Received January 5; accepted May 9, 1996

Abstract. We selected 33 unidentified IRAS sources based on the following criteria: i) galactic latitude more than 2°, ii) have flux density higher than 1 Jy at 12 microns, iii) have good fluxes at 12, 25, and 60 microns with flux quality factor = 3, iv) and are in the declination zone between +60° and −50°. We identified the optical counterparts of these sources on the POSS, ESO, and SERC sky survey prints. Out of the 33 sources studied by us, 30 have optical counterparts which are stellar in appearance. We have also made BVRI CCD photometry of the optical counterparts of these sources. The IRAS colours and optical photometry suggests that IRAS 00408 + 5933, 02408 + 5458, 04101 + 3103, 04278 + 2253, 04296 + 3429, 04386 + 5722, 05089 + 0459, 05113 + 1347, 05245 + 0022, 06403 − 0138, 07430 + 1115, 08005 − 2356, 09032 − 3953, 09370 − 4826, and 14429 − 4539 are most likely late type post-AGB stars with cold detached circumstellar envelopes and the rest are most likely AGB stars with dust shells.

Key words: stars: AGB, post-AGB — stars: evolution — stars: circumstellar matter — infrared: stars

1. Introduction

The Infrared Astronomical Satellite (IRAS) Point Source Catalog (PSC) contains a large number of point sources that emit strongly in the $12 - 100$ μm range, but have no counterparts in other astronomical catalogues. These are generally referred to as 'unidentified' or unassociated sources. All these sources appear to have circumstellar envelopes (CSE) of gas and dust. We have chosen thirty-three such 'unidentified' sources to study their evolutionary characteristics. The sources selected meet the following criteria: i) are still 'unidentified', ii) are at a galactic latitude $|b| \geq 2°$ (to minimise the problems arising from source confusion), iii) have good quality flux densities (Quality Factor = 3) in the first three bands of the IRAS Survey, iv) have a flux density higher than 1 Jy at 12 μm, and v) are in the declination zone between +60° and −50° to ensure ease of observation from Kavalur, India (longitude = 78.83°E and latitude = 12.57°N).

Hu et al. (1993) found several post-AGB stars using the IRAS colour criteria. Habing et al. (1987) pointed out that non-variable OH/IR stars, located to the red side of the region occupied by the AGB stars in the IRAS colour-colour diagram, are proto-planetary nebula (PPN) candidates. In recent years evidence has grown that a number of high latitude supergiants with circumstellar dust shells and far-IRAS colours similar to planetary nebulae may in fact be post-AGB stars (e.g. Parthasarathy & Pottasch 1986). Quite a number of unidentified IRAS sources with IRAS colours similar to planetary nebulae have been found to be PPN candidates (Hrivnak et al. 1988, 1989; Likkel et al. 1987, 1991; van der Veen et al. 1989; Manchado et al. 1989; Garcia-Lario et al. 1990).

There are approximately 2300 IRAS sources in the PSC that meet the selection criteria described above. In this paper we included the sources for which we could get photometric observations in B, V, R, I bands. The number of photometric nights at Vainu Bappu Observatory, Kavalur are very few. We could carry out photometric observations of about 33 sources within the allotted observing time. We will continue to study the remaining sources.

In this paper we report an analysis of IRAS and optical photometric data of 33 unidentified IRAS sources. The sources were selected based on the above mentioned criteria. Out of the 33 sources studied by us, 30 have optical counterparts. The *BVRI* CCD photometric observations are presented for most of these stars.

2. Observations

2.1. Optical identification

We carried out a search for the optical counterparts of the selected sources using POSS, ESO and SERC Sky Survey prints and adopting a procedure similar to that outlined by Ghosh et al. (1984). The optical candidate of the IRAS source is the one inside the IRAS error ellipse. The HST Guide Star Catalog (hereafter GSC; Lasker et al. 1990; Jenkner et al. 1990) was also searched to find the optical

Send offprint requests to: K.V.K. Iyengar

Table 1. IRAS and Optical position of programme sources

No.	IRAS Name	IRAS position RA(1950)			Dec			Optical position RA(1950)			Dec			GSC J	V
		(h)	(m)	(s)	(°)	(′)	(″)	(h)	(m)	(s)	(deg)	(′)	(″)		
1	00408+5933	00	40	49.4	+59	33	51	00	40	49.1	+59	33	48		9.81[b]
2	02408+5458	02	40	49.1	+54	58	35								
3	04101+3103	04	10	10.2	+31	03	10	04	10	10.4	+31	03	11		10.14[b]
4	04179+4145	04	17	57.3	+41	45	11	04	17	57.9	+41	45	13		
5	04184+2008	04	18	29.7	+20	08	56	04	18	29.4	+20	08	55		14.38[a,b]
6	04278+2253	04	27	50.2	+22	53	41	04	27	50.4	+22	53	43		14.62[b]
7	04296+3429	04	29	40.3	+34	29	53	04	29	40.6	+34	29	54		13.67[b]
8	04386+5722	04	38	38.2	+57	22	11	04	38	36.9	+57	22	09		12.25[b]
9	05067+2942	05	06	43.4	+29	42	49	05	06	43.4	+29	42	52		
10	05089+0459	05	08	56.6	+04	59	50	05	08	56.7	+04	59	50		14.08[a,b]
11	05113+1347	05	11	18.1	+13	47	04	05	11	18.0	+13	47	03		12.13[e]
12	05235+1129	05	23	34.4	+11	29	01	05	23	34.4	+11	29	01		12.08[e]
13	05245+0022	05	24	30.9	+00	22	40	05	24	31.3	+00	22	39	10.29[c]	10.06[b]
14	06403-0138	06	04	19.5	-01	38	05								
15	06426-0825	06	42	42.0	-08	25	09	06	42	42.2	-08	25	08		
16	06510+1200	06	51	05.9	+12	00	16	06	51	06.0	+12	00	14		12.99[e]
17	07430+1115	07	43	04.2	+11	15	46	07	43	05.8	+11	15	40		12.03[b]
18	07593-1452	07	59	20.4	-14	52	36	07	59	20.9	-14	52	37	13.44[c]	
19	08005-2356	08	00	32.5	-23	56	16	08	00	32.6	-23	56	15	13.11[c]	
20	08235-4747	08	23	32.6	-47	47	57	08	23	33.3	-47	48	03	14.26[a,c]	
21	09032-3953	09	03	12.4	-39	53	10	09	03	12.8	-39	53	25		
22	09370-4826	09	37	03.5	-48	26	34	09	37	03.1	-48	26	28		
23	12384-4536	12	38	29.9	-45	36	58								
24	12387-3717	12	38	43.9	-37	17	56	12	38	44.2	-37	17	57	12.10[a,c]	
25	14429-4539	14	42	54.9	-45	39	33	14	42	54.8	-45	39	31	14.23[a,c]	
26	14512-4746	14	51	15.6	-47	46	29	14	51	15.1	-47	46	28	9.69[c]	8.62[d]
27	15269-4400	15	26	59.3	-44	00	17	15	26	59.1	-44	00	16	12.26[c]	
28	17173-4632	17	17	23.8	-46	32	30	17	17	23.5	-46	32	30		11.87[d]
29	17174-4641	17	17	25.0	-46	41	09	17	17	25.1	-46	41	10		10.86[d]
30	17201-4613	17	20	11.3	-46	13	50	17	20	10.9	-46	13	51		9.05[d]
31	17318-3606	17	31	53.1	-36	06	42	17	31	53.3	-36	06	42		10.39[d]
32	18123+0511	18	12	21.7	+05	11	56	18	12	21.7	+05	11	57		10.10[a,b]
33	18599+2246	18	59	54.9	+22	46	11	18	59	55.7	+22	46	18		8.49[b]

[a] The values listed refer to the mean values of magnitudes when measurements are available from more than one sky survey plate in the same band.
Sky plates from which GSC magnitudes have been obtained:
[b] Palomar V1
[c] SERC J
[d] SERC V
[e] Palomar V4.

counterpart for the programme sources. The GSC contains stars in the magnitude range 6 to 15. We were able to find the blue and/or V magnitudes for many of these sources from GSC. In Table 1 we list the Serial Number of the source, its IRAS name, IRAS position, optical position of its counterpart determined from our search, the blue and or V magnitude from GSC (where the IRAS source had a counterpart in GSC), and the sky plate from which the GSC magnitude was obtained.

2.2. IRAS data on the programme sources

We present in Table 2 the far-infrared data on the programme sources taken from IRAS PSC (1988). The table contains for each source in columnwise sequential order, the serial number of the source, its IRAS name, its flux densities in Janskys in the four IRAS bands at 12, 25, 60 and 100 μm (when the quality factor is 2 or higher), the Variability Index (Var), and the Low Resolution

Table 2. IRAS PSC data on the programme sources

No.	IRAS Name	$F_\nu(\lambda)$ in Jy				Var	LRS
		12 μm	25 μm	60 μm	100 μm		
1	00408+5933	11.78	10.89	7.39	8.27	0	1
2	02408+5458	11.70	20.81	7.28	2.94	8	-
3	04101+3103	2.98	6.80	5.27	3.44	2	-
4	04179+4145	29.84	8.04	1.87	-	9	44
5	04184+2008	16.00	5.22	0.95	-	9	-
6	04278+2253	10.35	12.28	8.09	8.23	2	-
7	04296+3429	12.74	45.94	15.45	-	1	-
8	04386+5722	17.97	22.99	4.39	-	0	-
9	05067+2942	19.02	6.18	1.37	-	7	15
10	05089+0459	7.37	21.89	11.10	3.78	1	-
11	05113+1347	3.78	15.30	5.53	-	1	-
12	05235+1129	5.40	8.58	13.88	23.43:[a]	1	-
13	05245+0022	1.31	3.28	2.48	1.62	1	-
14	06403-0138	13.53	18.47	5.09	2.44:[a]	9	-
15	06426-0825	19.39	5.57	0.97	-	9	-
16	06510+1200	10.52	2.80	0.56	-	0	13
17	07430+1115	7.68	29.93	10.67	2.53	0	-
18	07593-1452	12.91	3.49	0.76	-	9	01
19	08005-2356	17.96	51.80	29.83	10.35	1	-
20	08235-4747	10.19	2.57	1.07	-	0	01
21	09032-3953	20.38	125.88	92.31	28.65	0	50
22	09370-4826	10.82	30.14	14.16	5.41	0	01
23	12384-4536	170.86	152.99	26.47	6.82	2	24
24	12387-3717	96.49	61.36	7.67	2.63	0	-
25	14429-4539	14.62	33.30	13.64	2.91	1	-
26	14512-4746	14.28	4.25	0.62:[a]	-	1	16
27	15269-4400	67.99	47.88	4.37	-	1	28
28	17173-4632	10.58	1.39	1.21:[a]	-	3	-
29	17174-4641	82.38	59.17	8.98	-	1	28
30	17201-4613	68.10	29.83	5.39	-	5	15
31	17318-3606	53.08	23.04	3.62	-	5	15
32	18123+0511	10.72	11.02	4.21	-	0	14
33	18599+2246	12.99	3.73	0.75	-	0	17

[a] The symbol : by the side of the flux densities indicates their IRAS Quality Factor to be 2.

Spectrometer (LRS) spectral classification. The Variability Index measures the probability that the source observed by IRAS is variable as determined by multiple 12 and 25 μm measurements. It is seen from the data in Table 2 about half of the sources have flux densities monotonically decreasing with wavelength, while the remaining sources have their flux densities peaking at 25 μm, except in the one case where it peaks at 60 μm or beyond. The 12 μm flux density of the former sources is generally higher than 10 Jy, whereas the flux density of some of the latter sources is less than 10 Jy. Generally the sources in the former group are on an average brighter than sources in the latter group at 12 μm by several times.

Low Resolution Spectra (LRS) are available for 15 of the programme sources (Joint IRAS Science Working group 1986). Of the seventeen sources in the group $F_\nu(12\ \mu\text{m}) < F_\nu(25\ \mu\text{m}) < F_\nu(60\ \mu\text{m})$ thirteen have LRS spectra. Only three of the sources in the group $F_\nu(12\ \mu\text{m}) < F_\nu(25\ \mu\text{m}) > F_\nu(60\ \mu\text{m})$ have LRS spectra. The IRAS data on the LRS spectral classification of these sources is presented in Table 2.

2.3. $BVRI$ photometry of optical candidates of IRAS sources

The photometric observations of 'unidentified' IRAS sources were carried out using the CCD camera attached to the 1.02-m telescope of the Vainu Bappu Observatory (VBO), Kavalur on several nights. The CCD camera for these observations uses a Thomson CSF TH7882 CCD chip (384×576 pixels^2), which has a special coating for providing enhanced ultraviolet sensitivity. It is mounted in a liquid-nitrogen cooled dewar. The CCD in its imaging

mode at the $f/13$ Cassegrain focus of the 1.02-m telescope of VBO (at a scale of $0''.357$ pixel^{-1}) covers a total field of 137 arcsec $\times$ 206 arcsec. We used standard B, V, R and I filters to carry out the photometric observations.

The photometric observations reported here were carried out on several nights during the period January 1992 to March 1995. The extinction coefficients were determined each night by observing photometric standard stars. On those nights when enough measurements were not available to obtain the extinction coefficients the mean extinction coefficients valid for VBO, Kavalur were used. The photometric data were reduced using the tasks 'ccdred' routines of the IRAF package. The "DAOPHOT" package was used to determine the magnitude of the programme sources. In one or two cases where the images of the optical candidates were not well isolated, we used "DAOPHOT" for images in crowded fields to extract their magnitudes. These were then corrected for extinction due to air mass (at the observed altitude) to obtain the instrumental magnitudes and then converted to standard magnitudes (Johnson system) using the transformation coefficients for the filter system in use. The probable error in the magnitudes listed in Table 3 is $\pm 0^{\rm m}.05$, which is for the full sample. In Table 3, we list in sequential order, the serial number of the source, its IRAS name, B, V, R and I magnitudes from the present observations and the date of observation. In Fig. 1 we present a plot of $V-I$ versus $B-V$ for the sources for which we have $BVRI$ magnitudes from our measurements.

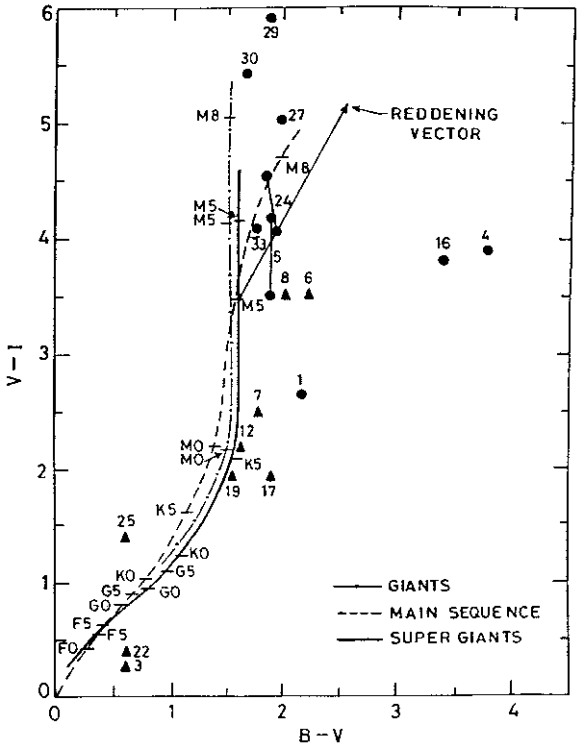

Fig. 1. $[V-I]$ versus $[B-V]$ colours for the sources for which we have B, V and I magnitudes from our photometric measurements. The numbers beside the points identify the sources of our study. The points • refer to sources with $F_\nu(12\ \mu\text{m}) < F_\nu(25\ \mu\text{m}) < F_\nu(60\ \mu\text{m})$ and points Δ refer to sources with $F_\nu(12\ \mu\text{m}) < F_\nu(25\ \mu\text{m}) > F_\nu(60\ \mu\text{m})$. The thick line, dot-dashed line and the dashed line show the dependence of $[V-I]$ versus $[B-V]$ for supergiants, giants and Main-sequence stars, respectively. The tick marks on these curves indicate the location of stars of different spectral type and luminosity classes. The reddening vector for a star of spectral type and luminosity M5V is also indicated

2.4. Classification of the programme sources according to their evolutionary status

van der Veen & Habing (1988, hereafter VH) carried out a study of the IRAS sources with CSE from an evolutionary point of view. They classfied the IRAS sources into ten different regions based on their location in the $[25-60]$ versus $[12-25]$ colour-colour diagram. In their notation $[25-60]$ and $[12-25]$ refer to $2.5\log(F_\nu(60)/F_\nu(25))$, and $2.5\log(F_\nu(25)/F_\nu(12))$ respectively, where the $F_\nu(\lambda)$'s are the IRAS flux densities at 60, 25, and 12 μm uncorrected for colour dependence. Stars with oxygen-rich envelopes form a sequence in this colour-colour diagram and has been interpreted as an evolutionary sequence of mass loss rate (Olnon et al. 1984; Bedijn 1987; van der Veen & Habing 1988); as a sequence of increasing initial masses (Epchtein et al. 1990); and as due to the combined effects of increasing mass loss rate and also increasing initial stellar masses (Likkel 1990). VH show that the evolutionary track of most of these stars in the $[25-60]$ versus $[12-25]$ colour-colour diagram is a single function of $[12-25]$ colour. This track passes through regions II, IIIa, IIIb and IV of VH. The envelope becomes thicker and cooler along this track as one moves from region II towards region IV; also there is an increase in variability, thought to be due to simultaneous occurence of pulsation and mass loss. However, there are other stars with CSE that populate a much wider area of this colour-colour diagram; some of these are due to carbon stars that have cooler envelopes due to the higher emissivity of carbon dust in their envelopes. These populate the upper regions of IIa and region VII of the VH diagram. Stars with a strong 60 μm excess (corresponding to cold dust) populate regions VIa and VIb. This can arise from discontinuities in the mass loss history of the star and due to the dust having moved farther away from the star. Protoplanetary Nebulae (PPN) and Planetary Nebulae (PN) are mostly found in regions IV and V where stars with very cold CSE's are situated. Thus, the VH diagram serves as a useful tool for obtaining preliminary information on the evolutionary status of stars with circumstellar envelopes. We present in Fig. 2 the programme sources on the VH diagram to classify them according to their evolutionary status.

Table 3. $BVRI$ magnitudes of the programme sources

No.	IRAS Name	B	V	R	I	Date of obsn.[a]
1	00408+5933	13.06	10.87	9.32	8.21	921227
	" "	13.07	11.14			930202
3	04101+3103	10.81	10.22	10.33	9.94	950302
4	04179+4145		14.00		11.53	920111
	" "	17.92	14.13	12.28	10.25	921226
5	04184+2008	13.42	11.54	9.12	8.03	920124
	" "	12.90	10.96			921226
	" "	15.5	14.1	11.6		941229
6	04278+2253	18.69	16.44	14.50	12.94	921227
7	04296+3429	16.14	14.34	12.97	11.83	921227
	" "	15.64	14.24	13.20		941229
8	04386+5722	14.90	12.85	11.34	9.34	930202
9	05067+2942[b]			16.55	14.07	920101
	05067+2942[c]		15.52	14.25	12.65	920101
	05067+2942[b]			18.43	15.45	921226
	05067+2942[c]	16.46	14.89	14.18	13.33	921226
10	05089+0459		14.32	12.68	11.62	930202
12	05235+1129	14.64	12.99	11.73	10.76	921227
15	06426-0825				¡15	920308
	" "			16.8	14.6	921226
16	06510+1200		12.24	10.23	8.35	920308
	" "	16.69	13.28	10.85	9.47	921227
17	07430+1115	14.32	12.40	11.48	10.50	921226
18	07593-1452		11.36	9.57	8.73	920124
19	08005-2356	13.07	11.52	10.62	9.58	921226
	" "		11.78	10.47	9.56	921227
20	08235-4747		12.07	9.88	8.00	920308
21	09032-3953			16.3	15.9	930202
22	09370-4826	14.70	14.07	14.01	13.66	950302
24	12387-3717	12.75	10.80	7.73	6.75	920124
	" "	12.75	10.85	9.15	6.30	921226
25	14429-4539			12.84	12.07	930202
	" "	14.09	13.46	13.09		950302
27	15269-4400	13.59	11.56	9.00	6.53	920308
	" "	11.94	11.30	10.65		950302
29	17174-4641	13.32	11.40	8.34	5.48	920308
30	17201-4613	11.25	9.53	6.77	4.07	920308
33	18599+2246	10.77	8.97	6.88	4.87	920308

[a] Format: yymmdd
[b] The faint component of the optical counterpart of IRAS 05067+2942.
[c] The bright component of the optical counterpart of IRAS 05067+2942.

3. Analysis of the data and comments on individual sources

We did not find any optical counterpart in either the J/P and/or V/R prints of the Sky Survey for IRAS sources $02408+5458, 06403-0138$ and $12384-4536$. We found an optical counterpart for IRAS sources $04179+4145, 04278+2253$, $06426-0825$, $06510+1200$ and $07593-1452$ on only the POSS R prints. In the case of IRAS 07430+1115 the optical counterpart is found to be on the edge of the IRAS error ellipse. Our finding charts do not show the optical counterpart of the IRAS source $09032-3953$, although an extremely faint one appears on the ESO/SERC print (due to difficulties in copying these survey prints which are enclosed in plastic sheets). We group sources occuring in the same region of the VH diagram together and then discuss selected sources in the order of their increasing serial number in each region. For some of the sources we have shown in Fig. 3 flux distribution curves based on optical near IR and IRAS data.

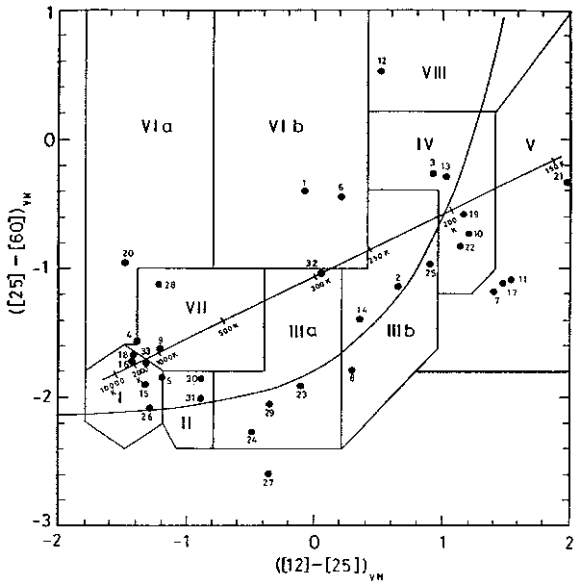

Fig. 2. Diagram showing the regions in the colour-colour plot of $[25-60]$ versus $[12-25]$ that separate different types of stars with circumstellar envelopes of dust and gas (adopted from van der Veen & Habing 1990; VH). The colours $[25-60]$ and $[12-25]$ are as defined by VH. The evolutionary track is indicated by the curve (thick line) $([25-60]) = -2.15 + 0.35 \times \mathrm{e}^{1.5([12-25])}$ which represents the observed colours very well for $-1.1 < ([12-25]) < 1.3$. The thin line shows the loci of black bodies with temperatures ranging from 10 000 K to 150 K with specific values shown at the tick marks on the line. The solid points indicate the position of the programme objects to indicate their state of evolution. The numbers beside the points identify the different sources as listed below. The programme sources are seen to be distributed over almost the entire region of the VH diagram. However, except for the six stars in region I of the VH diagram, the rest appear evolved to different degrees

3.1. Sources in region I

IRAS 04184+2008, IRAS 06462−0825, IRAS 06510+1200, IRAS 07593−1452, IRAS 14512−4746, IRAS 18599−2246 are in the region I of VH diagram (Fig. 2). The sources in this region are mostly due to the radiation from the photospheres. There is very little contribution to the IRAS fluxes from the circumstellar dust around these stars. The IRAS data does not indicate for the presence of dust envelopes around these stars.

5 IRAS 04184 + 2008

We have carried out $BVRI$ photometric observations of this source on three different nights viz., 920124, 921226 and 941229. The star is found to be brighter by about 2.5 magnitudes in V at epochs 920124 and 921226 compared to that at epoch 941229. It thus appears to be variable at the optical wavelengths also. Its position in the $V-I$ versus $B-V$ colour-colour diagram (Fig. 1) indicates it to be a star of spectral type M5 or later. Stephenson (1986), assigns a spectral type M6 and $V \geq 13.5$ from an examination of its spectrum in the $5000-6800$ Å region obtained at a dispersion of about 1000 Å mm^{-1} at H_α.

16 IRAS 06510 + 1200

The large differences in the VRI data at the two epochs of our observation suggest that it is variable at the optical wavelengths even though its IRAS variability index indicates that it is unlikely to be a variable at the far-infrared wavelengths. Its IRAS $[12-25]$ and $[25-60]$ colours and LRS spectrum indicate it to be either a 'Bright star' or a carbon-rich star. The position of this star in the $V-I$ versus $B-V$ colour-colour diagram (see Fig. 1) shows that it is highly reddened and that a significant fraction of its reddening is perhaps due to circumstellar dust.

26 IRAS 14512 − 4746 (CD -47 9519)

The $B-V$ value indicates it to be a star of spectral type G8Ia, or K0III or K4V. Its $[12-25]$ and $[25-60]$ colours and LRS spectrum indicate it to be an oxygen-rich star. It is identified with CD-47 9519 , with B and V magnitudes of 11.1 and 9.3 respectively, and a spectral type M5III (Simbad database).

3.2. Sources in region II

IRAS 17201 − 4613, IRAS 17318 − 3606 are in the region II of VH diagram (Fig. 2). Sources in this region have thin oxygen rich circumstellar envelopes. IRAS 17201 − 4613 is identified with HD 157144 ($V = 9.2$, $B = 10.9$, M6III).

3.3. Sources in region IIIa

Sources in the region IIIa of VH diagram (Fig. 2) are characterized by moderately-thick oxygen rich circumstellar envelopes. Sources in the region IIIb show thick oxygen rich circumstellar envelopes and sources in region IV are characterized by very thick oxygen rich circumstellar envelopes. According to the definition of van der Veen & Habing (1988), most cold AGB circumstellar envelopes are in regions IV, IIIb and coldest part of IIIa and protoplanetary nebulae are in region V. Among the circumstellar envelopes, the coldest ones are: i) AGB circumstellar envelopes with large mass-loss rates which are optically thick in the near infrared and emitting most of their energy in the far infrared. These are most likely to be the (very cold AGB, OH/IR stars and very cold carbon rich AGB stars) very late stages of the AGB with a large initial mass., ii) detached circumstellar envelopes associated with stars of intermediate spectral types believed to be in post-AGB stage or probably proto-planetary nebulae (Parthasarathy & Pottasch 1986). Again, they can be oxygen rich or carbon rich, with various mass-loss rates.

The sources described below which are in regions IIIa, IIIb, IV and V are most likely very cold AGB OH/IR

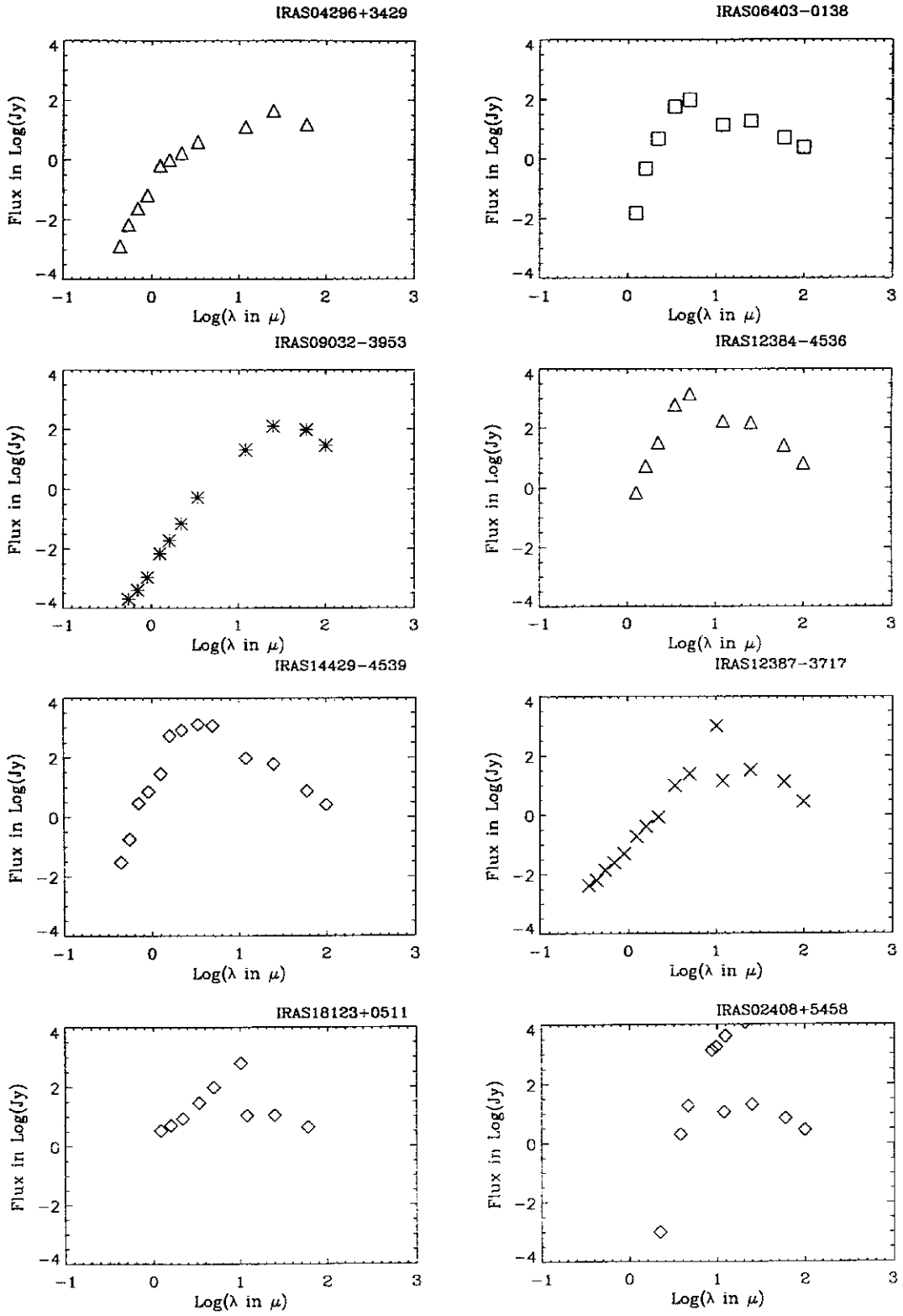

Fig. 3. The flux distribution of some of the sources listed in Table 1

stars, or very cold carbon rich AGB stars and post-AGB stars.

23 IRAS 12384 − 4536

We did not find any optical counterpart for this source in the Sky Survey prints. It was detected in the OH(1612 MHz) line by Lintel Hekkert et al. (1991), and was found to have a standard two peak spectrum with a velocity width of 26.1 km s^{-1} and a mean $V_{\rm LSR}$ of −36.3 km s^{-1} with flux densities of 4.50 mJy and 4.32 mJy for the blue and red shifted spikes. Nyman et al. (1992) carried out CO($J = 1-0$) observations of this source and detected it. They found it to have an expansion velocity of 8.1 km s^{-1} and an $V_{\rm LSR}$ of −38.6 km s^{-1}. Fouque et al. (1992), carried out near infrared photometric observations of this source and detected it in the $JHKLM$ bands. Its expansion velocity indicates that it is an AGB star undergoing mass loss. The LRS spectrum indicates that it is an oxygen rich circumstellar envelope. The flux distribution is shown in Fig. 3.

24 IRAS 12387 − 3717

Fouque et al. (1992) have carried out near infrared photometric observations of this source and obtain $JHKLM$ magnitudes. It is seen from a combination of our data with that of Fouque et al. (1992), that it has a $V-K$ of ~ 9.2 and hence highly obscured. It is perhaps also a variable at the optical wavelengths. The flux distribution is shown in Fig. 3.

29 IRAS 17174 − 4641

The LRS spectrum indicates that it is an oxygen rich circumstellar envelope. Nyman et al. (1992) could not detect CO($J = 1-0$) emission.

32 IRAS 18123 + 0511

This source has been detected in the OH(1612 MHz) line by Eder et al. (1988). Lawrence et al. (1990) have carried out infrared photometric observations of this source in the wavelength range $1-20$ μm, and give $JHKLMN$ magnitudes. They also list magnitudes of this source in a number of narrow bands around the 10 μm silicate feature and at 18 μm. The flux distribution is shown in Fig. 3.

3.4. Sources in region IIIb

2 IRAS 02408 + 5458

Blommaert et al. (1993) observed this source in the infrared in K, $L' = 3.80$ μm, $nbM = 4.64$ μm, 8.7 μm, 9.8 μm, 12.5 μm and Q bands and obtained magnitudes and classified it as a carbon star. The flux distribution is shown in Fig. 3.

8 IRAS 04386 + 5722

Blommaert et al. (1993) carried out near infrared photometric observations of this source. Its position in $B-V$ vs. $V-I$ is shown in Fig. 1.

14 IRAS 06403 − 0138

Photometric observations of this source in the $JHKLM$ bands were carried out by Blommaert et al. (1993). The flux distribution is shown in Fig. 3.

25 IRAS 14429 − 4539

This source is most likely a post-AGB star. Both Fouque et al. (1992), and Hu et al. (1993), report $JHKLM$ magnitudes of this source which are in very good agreement with one another. Optical data in combination with near-infrared photometric data yields a $V-K$ of 4.5 suggesting that it may be highly obscured object. Its flux distribution is shown in Fig. 3.

3.5. Sources in region IV

IRAS 04101+3103, IRAS 05089+0459, IRAS 05245+0022, IRAS 08005−2356 and IRAS 09370−4826 are in the region IV of VH diagram (Fig. 2). Several of these sources appear to be have thick oxygen rich circumstellar envelopes. The far infrared colours and flux distribution suggest that above mentioned sources are most likely post-AGB stars or proto-planetary nebulae similar to HD 161796 (Parthasarathy & Pottasch 1986). IRAS 08005 − 2356 and IRAS 09370 − 4826 were classified as proto-planetary nebulae by Slijkhuis (1992) and Hu et al. (1993) respectively. The LRS spectrum, IRAS colours and $BVRI$ photometry of IRAS 09370 − 4826 suggest that it is a post-AGB F supergiant.

3.6. Sources in Region V

Sources in region V of VH diagram (Fig. 2) is occupied by planetary nebulae and non-variable OH/IR stars with very cool circumstellar envelopes. some of the post-AGB stars and proto-planetary nebulae are also found in this region (van der Veen & Habing 1988). IRAS 04296 + 3429, IRAS 05113 + 1347, IRAS 07430 + 1115 and IRAS 09032 − 3953 are in region V. Some of these sources show 3.3 μm and 21 μm emission features indicationg that they are carbon rich.

7 IRAS 04296 + 3429

It is a carbon-rich star (Loup et al. 1993). It has been detected in the CO($J = 2-1$) line by Woodsworth et al. (1990) and by Omont et al. (see Loup et al. 1993), obtaining $V_{\rm exp}$ and $V_{\rm LSR}$ of 15.6 km s^{-1} and −62 km s^{-1} and 12.0 km s^{-1} and −66 km s^{-1}, respectively. This source has been classified as a PPN. Hrivnak et al. (1994), carried out H and K band low-resolution spectroscopic observations of this source. They also find dust features at 3.3, 3.4 and 21 μm and assign a spectral type G0Ia to this source. The

21 μm feature is suggested to be related to the polycyclic aromatic hydrocarbon (PAH) molecules commonly found in planetary nebulae (Buss et al. 1990).

Manchado et al. (1989), have detected this source in the $JHKL$ bands. We find its $V-K$ value to be 6.0 indicating that may be a highly obscured star. The observed flux distribution shown in Fig. 3.

11 IRAS 05113 + 1347

Hrivnak et al. (1994) carried out H, K and L band low-resolution infrared spectroscopic observations of this source. They detected H I and CO features in absorption and also the 3.3 μm feature (although weak). The available observations indicate that it is G type post-AGB supergiant.

17 IRAS 07430 + 1115

Hrivnak et al. (1994), carried out low-resolution infrared spectroscopy of this source. Our photometry and IRAS colours and flux distribution suggest that it is a post-AGB F or G supergiant.

21 IRAS 09032 − 3953

This source has been classified as a PPN by Hu et al. (1993). The CO line indicates a $V_{\rm LSR}$ of 36 km s^{-1} and an expansion velocity of 25 km s^{-1} (Loup et al. 1990). A search for the optical counterpart of this source on the ESO and SERC prints by us indicates an extremely faint optical object within the IRAS error ellipse, along with a brighter object towards the north-west boundry of the error ellipse. The finding chart of this source is given in Fig. 4. Hu et al. (1993), carried out $VRIJHKL$ photometric measurements of this object. On the basis of IRAS colours, LRS spectrum and photometry we conclude that it is a late type post-AGB supergiant. The observed flux distribution is shown in Fig. 3.

3.7. Sources in region VIa

Sources in the region VIa are characterized by non-variable stars, carbon-rich circumstellar envelopes with very cold dust at large distances. IRAS 04179 + 4145 and IRAS 08235 − 4747 are in region VIa (Fig. 2). The LRS spectrum of IRAS 04179 + 4145 also indicates that it is a carbon rich object.

3.8. Sources in region VIb

Sources in region VIb of VH diagram are occupied by variable stars, oxygen-rich circumstellar envelopes with very cold dust at very large distances. IRAS 00409 + 5933 and IRAS 04278 + 2253 are in region VIb (Fig. 2). Their location in $B-V$ vs. $V-I$ diagram suggest that they have very red colours. The IRAS flux distribution of these two sources is rather flat indicating temperature gradiant or multiple shells with a different dust temperatures.

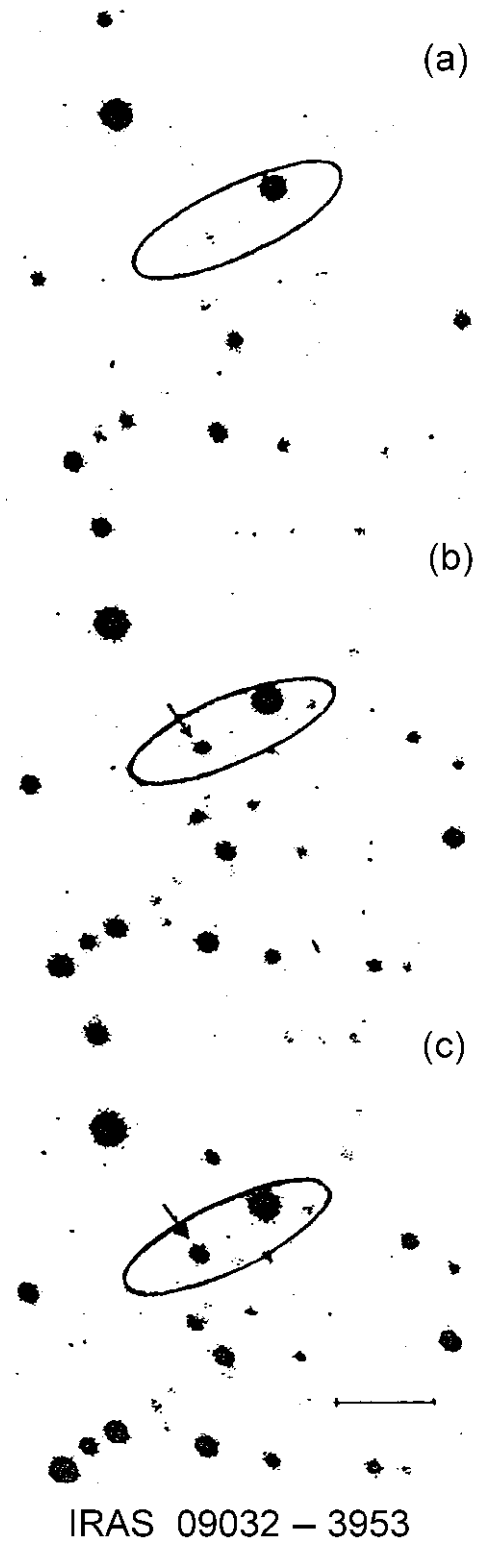

Fig. 4. CCD image of the region around IRAS 09032 − 3953 in the V, R and I photometric bands from observations of 2 Feb. 1993. North is up and East is to the left. The scale of the figure is indicated by the length of the line drawn in the R band image which corresponds to 20 arcsec

3.9. Sources in region VII

Sources in region VII of VH diagram are characterized by carbon-rich circumstellar envelopes. IRAS 05067 + 2942 and IRAS 17173 − 4632 occupy the region VII (Fig. 2).

9 IRAS 05067 + 2942

The location of this source in the VH diagram shows that it is likely to be in the AGB phase. We present in Fig. 5 the CCD images of this source in the V, R and I bands. The double images at the position of the IRAS source which are barely resolved on the POSS Sky Survey print E, appear well resolved on the R and I band CCD images. It is seen that the object indicated by the arrow (which is most likely to be the counterpart of the far-infrared source) on the R and I band CCD images does not show up in the V band image. The image of the brighter object close to the IRAS source also appears to get fainter as we go to shorter wavelength bands, but does not show such drastic changes in brightness as the one identified to be the counterpart of the IRAS source. Because of the close proximity of the brighter source to the weaker IRAS counterpart we used "daophot" in crowded fields to determine the magnitudes of this source in the different wavelength bands. Our $BVRI$ photometry of this source at two different epochs indicate that the source is a variable at the optical wavelengths also.

3.10. Source in region VIII

Sources in the region VIII of VH diagram are occupied by different sorts of obejects IRAS 05235 + 1129 is in the region VIII (Fig. 2). Our $BVRI$ photometric observations of these sources are in agreement with those obtained by Torres et al. (1995). The IRAS fluxes of this source show increasing flux from 12 μm to 100 μm similar to that of T Tauri stars, young stellar objects, compact H II regions and reflection nebulae.

3.11. Outside the regions defined by VH

27 IRAS 15269 − 4400

This source exhibits a 10^{μ}m silicate feature similar to the one in the spectrum of β Pictoris (Fajardo & Knacke 1995) which is a wide feature with two peaks at 9 and 11 μm. The spectral characteristics indicate that this type of emission originates from oxygen-rich circumstellar dust. They obtain a temperature of 300 K for the dust emission from this source after subtracting the contribution from the photospheric continuum. Our $BVRI$ photometry shows that it is a red object (Fig. 1).

4. Conclusions

Using a simple slection criteria we selected 33 unidentified IRAS sources. We carried out a search for the optical counterparts of the selected sources using the POSS, ESO,

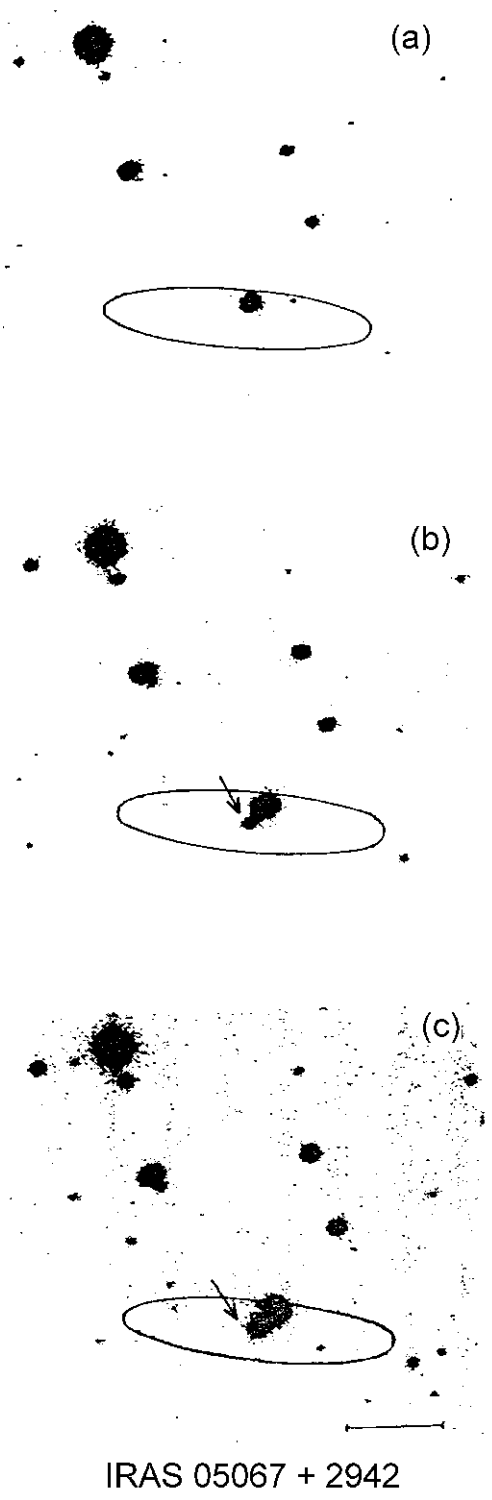

Fig. 5. CCD image of the region around IRAS 05067 + 2942 in the V, R and I photometric bands from observations on 11 Jan. 1992. North is up and East to the left. The scale of the figure is indicated by the length of the line drawn in the R band image which corresponds to 20 arcsec

and SERC sky survey prints. Out of the 33 sources we found optical counterparts for 30 sources which are stellar in appearance. We made CCD $BVRI$ photometric observations of the optical counterparts. Analysis of the IRAS and $BVRI$ colours suggests that 15 sources are most likely post-AGB stars.

Acknowledgements. We thank the observers Messrs. Muniyandi, Kuppuswamy and Dinakaran, at the 1.02-m telescope at VBO, Kavalur for kindly assisting us in these observations. We thank Prof. Ramsagar for kindly introducing us to the nuances of the "DAOPHOT" package for photometry. One of us (KVKI) thank the Council of Scientific and Industrial Research of the Government of India, for the award of an Emeritus Scientist Research Scheme which enabled these observations. KVKI also thanks the Smithsonion Institution for short - term visitor appointment to work at the Harward - Smithsonian center for Astrophysics, U.S.A. We thank Dr. T. Forveille for helpful comments.

References

Bedijn P.J., 1987, A&A 186, 136
Blommaert J.A.D.L, van der Veen W.E.C.J., Habing H.J., 1993, A&A 267, 39
Buss R.H. Jr., Cohen M., Tielens A.G.G.M., Werner M.W., Bregmann J.D., et al., 1990, ApJ 365, L23
Eder J., Lewis B.W., Terzian Y., 1988, ApJS 66, 183
Epchtein N., Le Bertre T., Lepine J.R.D., 1990, A&A 227, 82
Fajardo-Acosta S.B., Knacke R.F., 1995, A&A 295, 767
Fouque P., Le Bertre T., Epchtein N., Gugliemlo F., Kerschbaum F., 1992, A&AS 93, 151
Garcia-Lario P., Manchado A., Pottasch S.R, Suso J., Olling R., 1990, A&AS 82, 497
Ghosh S.K., Iyengar K.V.K., Rengarajan T.N., et al., 1984, MNRAS 206, 611
Habing H.J., van der Veen W.E.C.J., Geballe T., 1987, in: Late stages of stellar evolution, Kwok S. and Pottasch S.R. (eds.). Dordrecht, Reidel Publ., p. 91
Hrivnak B.J., Kwok S., Volk K.M., 1988, ApJ 331, 832
Hrivnak B.J., Kwok S., Volk K.M., 1989, ApJ 346, 265
Hrivnak B.J., Kwok S., Geballe T.R., 1994, ApJ 420, 783
Hu J.Y., Slijkhuis S., De Jong T., Jiang B.W., 1993, A&AS 100, 413
IRAS Point Source Catalog Version 2: 1988 Joint IRAS Science Working Group. Washington, D.C., U.S. Government Printing Office, PSC
Joint IRAS Science working Group, 1986, IRAS Catalogues and Atlases, Atlas of LOW Resolution Spectra, A&AS 65, 607
Jenkner H., Lasker B.M., Sturch C.R., et al., 1990, AJ 99, 2081
Lasker B.M., Sturch C.R., McLean B.J., et al., 1990, AJ 99, 2019
Lawrence G., Jones T.J., Gehrz R.D., 1990, AJ 99, 232
Likkel L., Omont A., Morris M., Forveille T., 1987, ApJ 173, L11
Likkel L., Forveille T., Omont A., Morris M., 1991, A&A 246, 153
Likkel L., 1990, in: From Miras to Planetary Nebulae: Which path for Stellar Evolution, Mennessier M.O., Omont A. (eds.). Editions Frontières, p. 258
Lintel Hekkert P., Caswell J.L., Habing H.J., Haynes R.F., Norris R.P., 1991, A&AS 90, 327
Loup C., Forveille T., Omont A., Paul J.F., 1993, A&AS 99, 291
Manchado A., Pottasch S.R., Garcia-Lario P., Esteban C., Mampaso A., 1989, A&A 214, 139
Nyman L.-Å., Booth R.S., Carlstrom U., et al., 1992, A&AS 93, 121
Olnon F.M., Baud B., Habing H.J., et al., 1984, ApJ 278, L41
Parthasarathy M., Pottasch S.R., 1986, A&A 154, L16
Slijkhuis S., 1992, Ph.D. thesis, Sterren Kundig Institut Anton Pannekoek, Amsterdam
Stephenson C.B., 1986, ApJ 301, 927
Torres C.A.O., Quast G., De La Reza R., Gregorio-Hetem J., Lepine J.R.D., 1995, AJ 109, 2146
van der Veen V.E.C.J., Habing H.J., 1988, A&A 194, 125
van der Veen V.E.C.J., Habing H.J., Geballe T.R., 1989, A&A 226, 108
Woodsworth A.W., Kwok S., Chan S.J., 1990, A&A 228, 503